Synergistic Active Sites on $SiO_2-Al_2O_3-TiO_2$ Photocatalysts for Direct Methane Coupling

Hisao Yoshida,* Norimitsu Matsushita, Yuko Kato, and Tadashi Hattori

Department of Applied Chemistry, Graduate School of Engineering, Nagoya University, Furo-cho, Chikusa-ku, Nagoya 464-8603, Japan

Received: February 24, 2003; In Final Form: May 27, 2003

The $SiO_2-Al_2O_3-TiO_2$ ternary oxide system exhibited high photocatalytic activity in the photoinduced direct methane coupling at room temperature to produce hydrogen and hydrocarbons such as ethane. The best $SiO_2-Al_2O_3-TiO_2$ sample containing 10 mol % of Al and 0.5 mol % of Ti marked about 20 times higher photocatalytic activity than the $SiO_2-Al_2O_3$ system reported previously. Al K-edge and Ti K-edge X-ray absorption near-edge structure (XANES) of the active $SiO_2-Al_2O_3-TiO_2$ samples indicated that both Al and Ti oxide species have a tetrahedral local structure in the active ternary samples. In the diffuse reflectance UV−vis spectra, the active samples showed additional absorption at 220−300 nm centered at 245 nm, which would be due to the interaction between the Al and Ti oxide species. The effective excitation wavelength of this photocatalyst for the photoinduced direct methane coupling was in good agreement with this additional photoabsorption. These results suggest that the pair sites consisting of the dispersed AlO_4 and TiO_4 species are responsible for the high activity of the $SiO_2-Al_2O_3-TiO_2$ photocatalyst in this reaction.

Introduction

To make an efficient utilization of natural gas, desired is the way to convert methane into more valuable chemicals. Higher hydrocarbons such as ethane, ethene, and so on are more useful for the chemical industry than methane. Direct methane coupling produces hydrogen and higher hydrocarbons such as ethane as follows.

$$2CH_4 \rightarrow C_2H_6 + H_2 \qquad \Delta G\ (298\ \mathrm{K}) = 68.6\ \mathrm{kJ/mol} \quad (1)$$

The large and positive ΔG value implies that the reaction hardly proceeds at mild conditions.

The oxidative coupling of methane (OCM) seems the effective reaction for producing higher hydrocarbons because the formation of water reduces the potential of products. Though extensive studies have been carried out worldwide, no catalysts could reach the principal criteria for industrial application of OCM,[1] because it is quite difficult to obtain the coupling products in high yield with less CO_x formation. The limits of the process have been essentially indicated.[2] A breakthrough for the methane conversion process is desired; the developments of other routes or other concepts are required.

Photocatalytic systems have the potential to promote difficult reactions and have been examined in both oxidative[3] and nonoxidative[4−6] systems for methane conversion. The performance of both systems examined, however, was not sufficient. In the oxidative system employing TiO_2 photocatalyst and oxygen, the complete oxidation mainly occurred,[3] while the conversion of methane was extremely low in nonoxidative systems employing V/SiO_2,[4] TiO_2,[5] and Mo/SiO_2.[6] We have recently proposed the photoinduced direct methane coupling over $SiO_2-Al_2O_3$[7−9] and zeolites[10] systems to produce both hydrocarbons and molecular hydrogen. This reaction proceeds even at room temperature without CO_x formation. In addition, it is noted that the photoenergy is stored in the products as chemical potential, which corresponds to ΔG in eq 1.

In the $SiO_2-Al_2O_3$ system, the highly dispersed AlO_4 species in the silica matrix are responsible for high selectivity to ethane.[7,11] The $SiO_2-Al_2O_3$ system exhibited obviously higher product yield than those in the other oxidative and nonoxidative photoinduced systems reported before.[3−6] However, the activity was not enough yet. One possible reason for the low activity of this system would be the low absorption efficiency of photoactive sites in the $SiO_2-Al_2O_3$ system, which shows only very small absorption band in UV−vis spectrum. On the other hand, the photocatalytic performance of highly dispersed TiO_4 species on silica materials for other reactions has been well studied,[12−21] and the high photoabsorption efficiency of charge transfer from O^{2-} to Ti^{4+} at Ti−O moiety is also well-known. It was expected that the addition of Ti species to the $SiO_2-Al_2O_3$ system might improve the photocatalytic activity. In the present study, we prepared the $SiO_2-Al_2O_3-TiO_2$ samples with various Al and Ti contents and carried out the spectroscopic characterization and the catalytic activity test in photoinduced direct methane coupling.

Experimental Section

Preparation of Samples. The $SiO_2-Al_2O_3-TiO_2$, $SiO_2-Al_2O_3$, and SiO_2-TiO_2 samples were prepared by sol−gel method as follows.[22] One mole of $Si(OC_2H_5)_4$ was first mixed with 5 mol of C_2H_5OH, and the mixture was stirred at room temperature for 1 h (the liquid A). The liquid B consisted of 5 mol of C_2H_5OH, 50 mol of H_2O, 0.02 mol of HNO_3, $(NH_4)_2[Ti(C_2O_4)_2]\cdot 2H_2O$, and $Al(NO_3)_3\cdot 9H_2O$ with the designed contents. This liquid B was added dropwise to the liquid A, and the fully mixed solution was stirred at room temperature for additional 1 h. The prepared sol was stirred at 353 K under the partial vacuum for a few hours until a wet gel was obtained. The wet gel was dried at 383 K and calcined in a flow of air at 773 K for 5 h.

* To whom correspondence should be addressed. Fax: +81-52-789-3193. E-mail: yoshidah@apchem.nagoya-u.ac.jp.

10.1021/jp034458+ CCC: $25.00
Published on Web 07/16/2003

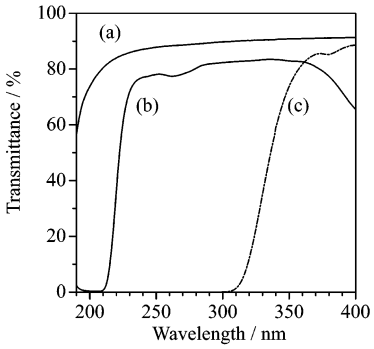

Figure 1. UV-vis transmission spectra of the employed filters: (a) water; (b) $CoSO_4$ aqueous solution; (c) UV-33.

$Al_2O_3-TiO_2$ was obtained by calcination of the hydroxide, obtained by coprecipitation of $(NH_4)_2[Ti(C_2O_4)_2]\cdot 2H_2O$ and $Al(NO_3)_3\cdot 9H_2O$ with 10% NH_4OH aqueous solution. The sample $TiO_2/SiO_2-Al_2O_3$, was prepared by the impregnation method; the sol−gel-prepared $SiO_2-Al_2O_3$ powder was impregnated with $(NH_4)_2[Ti(C_2O_4)_2]\cdot 2H_2O$ aqueous solution. The SiO_2 sample was prepared from $Si(OC_2H_5)_4$ by sol−gel method.[23] These samples were calcined in the flow of air at 773 K for 5 h. The Al_2O_3 sample was obtained by calcination of $Al(NO_3)_3$ at 773 K. The TiO_2 sample was a reference catalyst of Catalysis Society of Japan, JRC-TIO-4,[24] which is similar to P-25.

Some reference samples were employed for the X-ray absorption fine structure (XAFS) study. Titanium isopropoxide Ti(O-*i*Pr)$_4$ and anatase TiO_2 were commercial reagents, which are the references of tetrahedral TiO_4 and octahedral TiO_6 species, respectively. MFI-type aluminosilicate (JRC-Z5−25H,[24] $SiO_2/Al_2O_3 = 25$), as the reference of tetrahedral AlO_4 species, was supplied from the Catalysis Society of Japan. α-Al_2O_3, as the octahedral AlO_6 species, was prepared by calcination of aluminum hydroxide (boehmite) in air at 1773 K,[25] and the crystal structure was confirmed by X-ray diffraction.

Reaction Test. The reaction test was carried out in a closed quartz reaction vessel (68.0 cm^3).[26] The sample (1.0 g) was spread on the flat bottom of vessel (14.5 cm^2), and it was pretreated with 60 Torr (1 Torr = 133 Pa) of O_2 for 1 h at 1073 K, followed by evacuation for 1 h at 1073 K. Methane (99.95%) purchased was further purified by a vacuum evaporation before every use and introduced into the reactor. The initial pressure of methane (200 μmol) in the reactor was ca. 55 Torr. No oxidant molecules were introduced. The sample was irradiated by using a 250 W Xe lamp for 6 h. Under photoirradiation, the temperature of the sample bed was measured to be ca. 310 K. The formed H_2 was quantified by a gas chromatograph (GC) connected with a thermal conductivity detector (TCD). The hydrocarbons as coupling products and CO_2 in a gaseous phase were collected with a liquid-N_2 trap and analyzed by GC connected with a flame ionization detector (FID) and a TCD, respectively. Then, hydrocarbon products adsorbed on the sample at the reaction temperature were thermally desorbed by heating (573 K, 15 min), collected with liquid-N_2 trap, and analyzed by GC-FID.

Three UV-cut filters were employed to examine the effective wavelength toward the reaction. These UV−vis transmission spectra are shown in Figure 1. Water filter transmitted all wavelengths in UV regions. A glass filter (TOSHIBA UV-33) and a $CoSO_4$ aqueous solution filter transmitted above 310 and 210 nm, respectively.

Spectroscopic Characterization. Ti K-edge X-ray absorption near-edge structure (XANES) spectra were obtained at BL-9A station[27,28] of Photon Factory, Institute of Materials Structure Science, High Energy Accelerator Research Organization in Tsukuba (KEK-PF, Japan), with ring energy of 2.5 GeV and stored current of 300−450 mA. The spectra were recorded with a Si(111) double-crystal monochromator in a transmission mode or a fluorescence mode at room temperature. High-energy X-rays from high-order reflections were removed by a pair of flat quartz mirrors coated with Ni. The energy was defined by assigning the first characteristic peak of the Cu foil spectrum to 8978.9 eV.[29] The sample was pretreated at 1073 K with 60 Torr of O_2 for 1 h, followed by evacuation for 1 h, and sealed with a polyethylene film in dry atmosphere. The step angle of the monochromator scanning was 0.00135°, which corresponds to about 0.3 eV around 5000 eV.

Al K-edge X-ray absorption spectra were measured under vacuum ($<10^{-6}$ Torr) in a mode of total electron yields on BL-7A[30] at UVSOR of the Institute for Molecular Science in Okazaki (Japan) with a ring energy of 750 MeV and a stored current of 70−220 mA. A KTP(011) ($KTiOPO_4$, 2d = 10.95 Å) double-crystal monochromator[31] was used. The sample was put on the first Cu−Be dynode of the electron multiplier (−1.5 kV) by using adhesive carbon tape. The step angle of the monochromator scanning was 0.01°, which corresponds to about 0.3 eV at 1560 eV. The energy correction was done by the position of the peak due to tetrahedral AlO_4 of the reference sample, MFI-type aluminosilicate (H-ZSM-5).[25] XANES spectrum was normalized to the height of the edge jump after removal of contribution from absorption other than the K-edge absorption by the Al or Ti atom.

Diffuse reflectance UV spectra of samples were measured using JASCO V-570 UV/VIS/NIR spectrophotometer at room temperature. The samples were prepared at 1073 K with 60 Torr of O_2 for 1 h, followed by evacuation for 1 h, and their spectra were measured at room temperature without exposure to air.

Results

Photoinduced Direct Methane Coupling. Through the photoinduced direct methane coupling in the present study, hydrogen, ethane and a small amount of propane were formed in gaseous phase. In addition, C_{2-4} alkane and alkene products were adsorbed on the sample surface during the photoirradiation, and they were collected by thermal desorption process. No product was obtained without photoirradiation or without the sample oxides.

Table 1 shows the results of photoinduced direct methane coupling over some samples in various combinations of Si, Al, and Ti oxides. Over the SiO_2 sample (entry 1), the small amount of ethane was formed in gaseous phase. Over the Al_2O_3 sample (entry 2), in addition to the small amount of ethane and hydrogen in gaseous phase, the adsorbed products were also observed as reported previously.[8,9] The activity of the TiO_2 sample (entry 3) was higher than those of the SiO_2 and Al_2O_3 samples, although hydrogen was not detected. Over the $SiO_2-Al_2O_3$ (10 mol % Al), small amounts of ethane and hydrogen were formed in the gaseous phases (entry 4). It is previously reported that around 10−20 mol % of Al is suitable to obtain the high activity of the $SiO_2-Al_2O_3$ samples toward photoinduced direct methane coupling because the maximum amount of the highly dispersed AlO_4 species can exist as the active sites.[7] Although the SiO_2-TiO_2 (10 mol % of Ti) sample exhibited very low activity (entry 5), the SiO_2-TiO_2 (0.1 mol % Ti) sample produced small amounts of ethane and hydrogen in the gaseous phases (entry 6). This indicates that low Ti content in SiO_2-TiO_2 is suitable for this photoinduced reaction. The $Al_2O_3-TiO_2$ (entry 7)

TABLE 1: The Results of Photoinduced Direct Methane Coupling[a]

		content			yield of products					
entry	sample	Al, mol %	Ti, mol %	SA[b] (used), m^2/g	C_2H_6, C%[e]	C_3H_8, C%[e]	$C_{2+(ad)}$,[c] C%[e]	totalC_{2+}, C%[e]	H_2, μmol	$H_{2,calcd}$,[d] μmol
1	SiO_2	0	0	297	0.02	0.00	0.00	0.02	*g*	0.02
2	Al_2O_3	100	0	92	0.05	0.00	0.03	0.08	*g*	0.10
3	TiO_2	0	100	13	0.11	0.01	*g*	0.12	0.00	0.12
4	$SiO_2-Al_2O_3$	10	0	420	0.10	0.00	0.00	0.10	0.05	0.10
5	SiO_2-TiO_2	0	10	5	*g*	0.00	0.00	0.00	0.03	
6	SiO_2-TiO_2	0	0.1	47	0.09	*g*	0.00	0.09	0.11	0.09
7	$Al_2O_3-TiO_2$	99.9	0.1	170	0.43	0.01	0.26	0.70	1.10	0.91
8	$SiO_2-Al_2O_3-TiO_2$	10	0.1	311	1.56	0.14	0.07	1.77	2.69	1.91
9	$SiO_2-Al_2O_3-TiO_2$	10	0.5	251	2.07	0.25	0.15	2.47	3.54	2.76
10	$TiO_2/SiO_2-Al_2O_3$	10	0.1	441	0.57	0.01	0.01	0.60	0.70	0.60
11[f]	$SiO_2-Al_2O_3-TiO_2$	10	0.05	372	2.71	0.59	0.29	3.74	5.84	4.37

[a] Reaction time = 3 h; sample weight = 1.0 g; CH_4 = 200 μmol. [b] BET surface area of the samples after pretreatment at 1073 K for the reaction test. [c] C_{2+} products collected through the thermal desorption process. [d] Calculated from obtained coupling hydrocarbons based on stoichiometric reaction formula. [e] Based on initial amount of methane. [f] Reaction time 90 h, sample weight 0.3 g. [g] Trace.

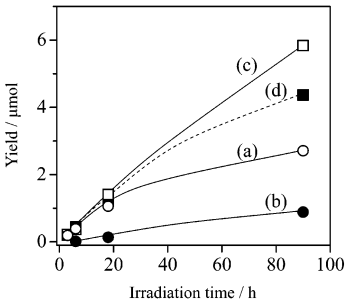

Figure 2. The time course of C_2H_6, C_3H_8, and H_2 yield in photoinduced direct methane coupling over $SiO_2-Al_2O_3-TiO_2$ ternary oxide (Al = 10 mol %, Ti 0.05 mol %): (a) C_2H_6; (b) C_3H_8; (c) H_2 experimental. The plot on the broken line (line d) shows the H_2 amount calculated from C_{2+} yield with stoichiometric formula. Initial amount of methane was 200 μmol. After 90 h reaction, 0.15 C% of C_4H_{10} and 0.30 C% of C_{2+ad} were also detected.

sample showed higher activity than the above binary oxides did. However, heat treatment of the sample was required to collect a part of hydrocarbons that remained on the sample.

On the other hand, the $SiO_2-Al_2O_3-TiO_2$ sample exhibited much higher product yields, especially ethane and hydrogen in gaseous phase (entries 8 and 9). Considering the low activities of the SiO_2-TiO_2 and $SiO_2-Al_2O_3$ samples (entries 4 and 6), it is indicated that the Ti and Al species synergistically functioned and this high activity was attained. In the present study, the maximum yields were shown over the sample including 0.5 mol % of Ti and 10 mol % of Al (entry 9). The activity of the sample prepared by impregnation method, $TiO_2/SiO_2-Al_2O_3$, was lower than that of the sol−gel sample (entry 10).

Figure 2 shows the time course of the product yields in the photoinduced direct methane coupling over the $SiO_2-Al_2O_3-TiO_2$ sample containing 10 mol % of Al and 0.05 mol % of Ti. The yield of coupling products monotonically increased with the photoirradiation time. In the early stage, ethane was predominantly formed. Then, propane appeared and increased with the photoirradiation time. After 90 h reaction, 0.15 C% of butane and 0.30 C% of adsorbed C_{2+} hydrocarbons were also detected, in addition to ethane and propane. These suggest that the reaction proceeded to grow the carbon chain successively, which is the same as the case of the $SiO_2-Al_2O_3$ system reported previously.[8] After 90 h photoreaction with the 0.05 mol % Ti sample, the methane conversion calculated from collected coupling products, 3.74 C% = 7.48 μmol, went up to 3 times higher than that of Ti in the sample, 2.53 μmol (Table 1, run 11). When we assumed that the number of the active sites corresponded to that of Ti atoms, the estimated turn over number (TON) exceeded unity at least, suggesting that this reaction occurs photocatalytically.[22]

Figure 2 shows also the hydrogen yield (curve c) experimentally obtained, as well as the calculated hydrogen yield (curve d) that was obtained from the amount of the all kinds of detected C_{2+} hydrocarbons assuming the stoichiometric formula. The hydrogen yield increased monotonically with the irradiation time, indicating that the coupling reaction or dehydrogenation of hydrocarbons or both proceeded continuously by photoirradiation. Although the calculated value almost agreed with the experimental hydrogen yield, it was slightly less than experimental value after the 90 h reaction. This deviation would come from the fact that a part of hydrocarbons adsorbed strongly could not be collected in the present heating condition after the photoinduced reaction and these are not included in the calculation. Each calculated value for reaction tests was listed in Table 1 as reference.

The photocatalytic activity of the $SiO_2-Al_2O_3-TiO_2$ system was much affected by the composition of Al and Ti, pretreatment temperature, and wavelength of irradiation light. The variation of the activity in the present photoinduced direct methane coupling with the contents of Al and Ti was systematically examined. The results were listed in Table 2. Almost all of the samples of $SiO_2-Al_2O_3-TiO_2$ with various contents showed the activity; ethane and hydrogen were produced. Some samples having large Al and Ti content did not show enough hydrogen formation, probably because side reaction occurred, for example, the photoreduction of the catalyst surface by produced hydrogen or oxidative methane coupling by lattice oxygen.

Figure 3 depicts the specific yield of ethane per surface area of the sample from the data from Table 2, because ethane was the main product in each case. In Figure 3, it is obvious that the sample with Ti = 0.5 mol % and Al = 10 mol % exhibited the highest yield. The same result is obtained even when the activity was directly compared on the ethane yield (C%) in Table 2. Among the samples of low Ti content from 0.1 to 1, the maximum ethane yield was obtained on the sample containing 10 mol % of Al. This optimum Al content is similar to the case of the $SiO_2-Al_2O_3$ system previously reported.[7]

The effect of pretreatment temperature before the reaction test was examined by using the $SiO_2-Al_2O_3-TiO_2$ sample with 10 mol % of Al and 0.5 mol % of Ti (Figure 4). The activity was very low after pretreatment at 673 K and slightly increased by pretreatment at 873 K. However, the evacuation at 1073 K drastically enhanced the yield. It was also reported in the SiO_2-

TABLE 2: The Results of Photoinduced Direct Methane Coupling over the $SiO_2-Al_2O_3-TiO_2$ Samples[a]

	content			C_2H_6 yield		total	H_2	
entry	Al, mol %	Ti, mol %	SA,[b] m^2/g	C%[c]	nmol/m^2 [d]	C_{2+}, C%[c]	yield, μmol	$H_{2,calcd}$,[e] μmol
1	1.0	0.1	77	0.10	1.32	0.11	0.14	0.11
2	1.0	0.5	58	0.08	1.37	0.08	0.13	0.087
3	1.0	1.0	104	0.17	1.59	0.19	0.37	0.19
4	1.0	2.9	91	0.27	2.98	0.28	0.33	0.33
5	1.0	4.8	148	0.36	2.45	0.37	0.43	0.39
6	10.0	0.1	311	1.56	5.02	1.63	2.69	1.91
7	10.0	0.25	227	1.57	6.94	1.63	2.70	1.86
8	10.0	0.5	251	2.07	8.25	2.22	3.54	2.76
9	9.9	1.0	260	1.45	5.58	1.55	2.06	1.84
10	9.5	4.8	125	0.18	1.41	0.19	0.15	0.19
11	33.3	0.1	228	0.49	2.17	0.49	0.54	0.50
12	33.2	0.5	216	0.48	2.22	0.48	0.46	0.51
13	33.0	1.0	207	0.32	1.56	0.32	0.29	0.33
14	31.7	4.8	207	0.14	0.66	0.15	0.03	0.15
15	66.6	0.1	172	0.32	1.85	0.33	0.29	0.34
16	66.4	0.5	148	0.28	1.91	0.29	0.17	0.30
17	66.0	1.0	188	0.32	1.72	0.34	0.13	0.38
18	63.5	4.8	206	0.17	0.82	0.18	0.00	0.19

[a] Reaction time = 3 h; sample weight = 1.0 g; CH_4 = 200 μmol. [b] BET surface area of the samples after pretreatment at 1073 K for the reaction test. [c] Based on initial amount of methane. [d] The yield normalized by the surface area. [e] Calculated from obtained coupling hydrocarbons based on stoichiometric reaction formula.

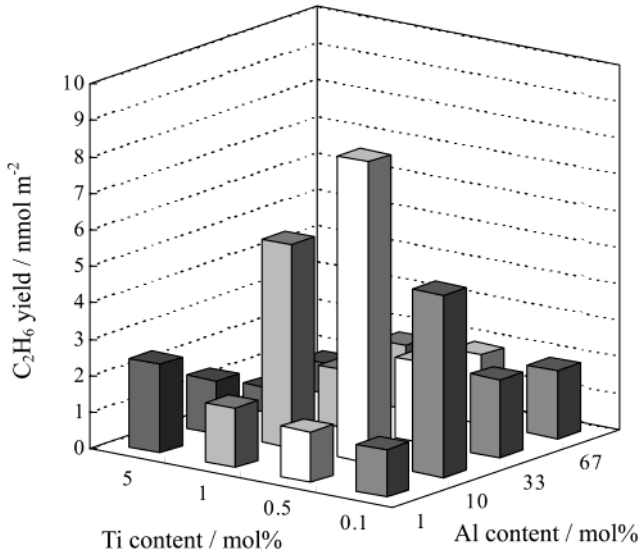

Figure 3. The ethane yield (per specific surface area) in photoinduced direct methane coupling over the $SiO_2-Al_2O_3-TiO_2$ samples with various Al and Ti contents. Sample weight was 1.0 g; pretreatment before the reaction test was carried out at 1073 K; initial amount of methane was 200 μmol; reaction time was 6 h.

Al_2O_3 system that the activity was increased by the higher temperature evacuation prior to the reaction.[8] Desorption of surface hydroxyl groups at high temperature would be related to the generation of the photocatalytic active sites.[8,11]

To clarify the effective wavelength of irradiation light for this photoinduced system, UV-cut filters (Figure 1) were employed to restrict the irradiation light. The results on the $SiO_2-Al_2O_3-TiO_2$ sample with 10 mol % of Al and 0.05 mol % of Ti are listed in Table 3. The photocatalytic reaction proceeded with the light transmitted through a water filter (entry 1). When a $CoSO_4$ aqueous solution filter (entry 2) was used, the yield slightly decreased. However, considering the difference between transmittance of water and that of the $CoSO_4$ aqueous solution in $\lambda > 210$ nm in Figure 1, ca. 90% and 80%,

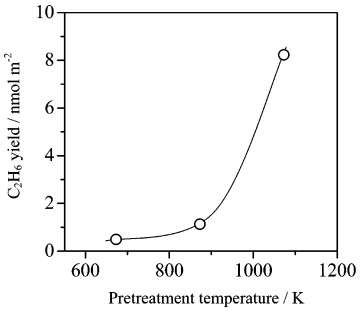

Figure 4. The effect of pretreatment temperature upon the ethane yield over the $SiO_2-Al_2O_3-TiO_2$ sample containing 10 mol % of Al and 0.5 mol % of Ti. Sample weight used was 1.0 g; initial methane amount was 200 μmol; reaction time was 6 h.

TABLE 3: The Results of Photoinduced Direct Methane Coupling with UV-Cut Filters[a]

			yield of products			
entry	filter	transmission light,[d] nm	C_2H_6, C%[c]	$C_{2+(ad)}$,[b] C%[c]	total C_{2+}, C%[c]	H_2, μmol
1	water	>190	0.15	0.01	0.16	0.18
2	$CoSO_4$	>210	0.11	0.01	0.12	0.13
3	UV-33	>310	*e*	0.00	*e*	0.00

[a] Sample weight = 0.3 g; Ti = 0.05 mol %; Al = 10 mol %; pretreated at 1073 K; CH_4 = 200 μmol; reaction time = 6 h. [b] C_{2+} products collected through the thermal desorption process. [c] Based on initial amount of methane. [d] See Figure 1. [e] Trace.

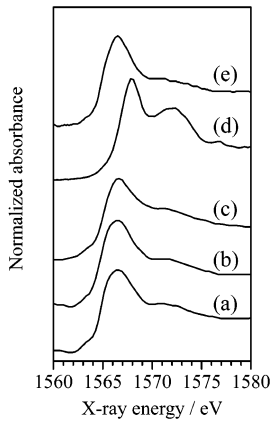

Figure 5. Al K-edge XANES spectra of sol−gel prepared $SiO_2-Al_2O_3-TiO_2$ containing 10 mol % of Al and various amount of Ti: (a) 0.1 mol %; (b) 0.5 mol %; (c) 4.8 mol %. As a reference, α-Al_2O_3 for octahedral AlO_6 (d) and ZSM-5 for tetrahedral AlO_4 (e) are also shown.

respectively, the yield with the $CoSO_4$ aqueous solution filter should be estimated as comparable to that with the water filter. This means that the light less than 210 nm was not effective for the reaction so much. On the other hand, the reaction did not proceed with an UV-33 glass filter (run 3). From these results, it is concluded that the effective wavelength of light was in the region of 210−310 nm for this photoinduced reaction.

Local Structure of the Al and Ti Sites. The XANES spectrum reflects the local coordination symmetry of the target atom. The local structures of the Al and Ti species in the $SiO_2-Al_2O_3-TiO_2$ samples were investigated by XANES spectra. Figure 5 shows Al K-edge XANES spectra of the representative $SiO_2-Al_2O_3-TiO_2$ samples (10 mol % of Al, 0.1−4.8 mol % of Ti) and the references. The white line peak at 1566 eV is assigned to the tetrahedral AlO_4 species, while the peaks at 1568 eV is assigned to the octahedral AlO_6 species.[25,32−35] For example, MFI-type aluminosilicate (AlO_4 tetrahedra) exhibited

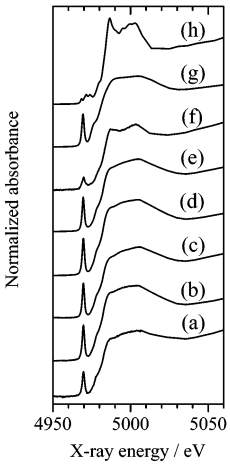

Figure 6. Ti K-edge XANES spectra of the sol−gel prepared $SiO_2-Al_2O_3-TiO_2$ samples containing 10 mol % of Al and various amount of Ti: (a) 0.1 mol %; (b) 0.25 mol %; (c) 0.5 mol %; (d) 1.0 mol %; and (e) 4.8 mol %. The XANES spectra of the $TiO_2/SiO_2-Al_2O_3$ sample prepared by impregnation method (f), $Ti(O^iPr)_4$ consisting tetrahedral TiO_4 (g), and anatase consisting of octahedral TiO_6 (h) were also shown as a reference.

a white line peak at 1566 eV (Figure 5e), while α-Al_2O_3 (AlO_6 tetrahedra) exhibited a peak at 1568 eV (Figure 5d). The $SiO_2-Al_2O_3-TiO_2$ samples that contain 10 mol % of Al exhibited a white line at 1566 eV, indicating that the tetrahedral AlO_4 species is dominant in these samples (Figure 5a−c). The slight change of the spectra shape among them might be due to the interaction with coexisting Ti atoms.

Figure 6 shows the Ti K-edge XANES spectra of the $SiO_2-Al_2O_3-TiO_2$ samples. It is well-known that the tetrahedral TiO_4 species exhibits a strong single preedge peak, while the preedge peak of the octahedral TiO_6 species is weak.[36,37] The position and intensity of the preedge peak also reflects the coordination symmetry.[36] Ti(O-*i*Pr)$_4$ consisting of tetrahedral TiO_4 exhibits a strong single preedge peak (Figure 6g); TiO_2 anatase including octahedral TiO_6 shows three weak preedge peaks (Figure 6h), as reported.[36,38] All of the spectra of $SiO_2-Al_2O_3-TiO_2$ samples prepared by the sol−gel method shown in Figure 6a−e were similar to that of Ti(O-*i*Pr)$_4$, and the energy positions of preedge peak were identical to each other. It is indicated that tetrahedral-coordinated TiO_4 was dominant in the sol−gel samples, even the high Ti content samples such as 4.8 mol % of Ti. On the other hand, the spectrum of the $TiO_2/SiO_2-Al_2O_3$ sample of 0.1 mol % Ti prepared by the impregnation method (Figure 6f) had a weaker single preedge and the clear first peak at postedge that is similar to anatase TiO_2 of octahedral TiO_6 species (Figure 6h). These indicate that the tetrahedral TiO_4 species was minor in the impregnated samples.

From these results on XANES spectra, it is clear that the major Al and Ti species in the photocatalytically active $SiO_2-Al_2O_3-TiO_2$ samples are the tetrahedral AlO_4 and TiO_4 species.

Electronic Structure of the Photoactive Sites. The electronic structure of photoabsorption sites, which might be deeply related to the photocatalytic activity, can be characterized by UV−vis spectroscopy. Diffuse reflectance UV−vis spectra of the samples and references are shown in Figures 7 and 8.

Figure 7A shows the spectra of the $SiO_2-Al_2O_3-TiO_2$ samples containing 0.1 mol % of Ti with various Al content. The $SiO_2-Al_2O_3$ sample exhibited a very small band around 220−320 nm (Figure 7a) as reported.[7] The SiO_2-TiO_2 sample containing 0.1 mol % of Ti exhibited a large and narrow absorption band below 260 nm with the maximum around 200

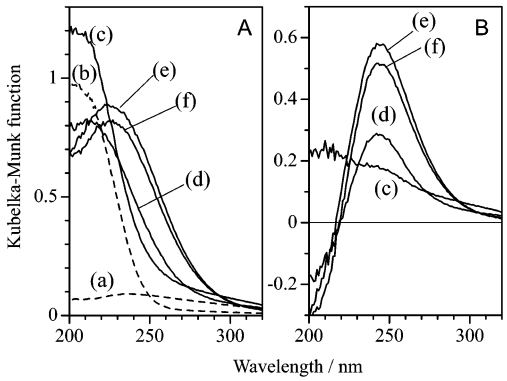

Figure 7. Diffuse reflectance UV−vis spectra (A) of the (a) $SiO_2-Al_2O_3$ (Al = 10 mol %), (b) SiO_2-TiO_2 (Ti = 0.1 mol %), and $SiO_2-Al_2O_3-TiO_2$ samples containing 0.1 mol % of Ti and (c) 1.0, (d) 10, (e) 33, and (f) 67 mol % of Al and (B) difference spectra obtained by the subtraction of spectrum b from the indicated spectra.

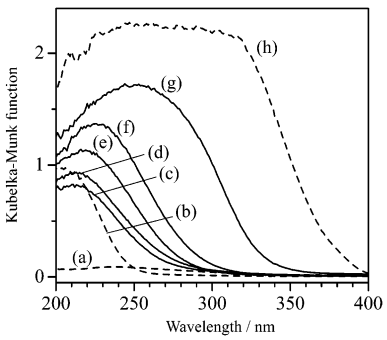

Figure 8. Diffuse reflectance UV−vis spectra of the (a) $SiO_2-Al_2O_3$ (Al = 10 mol %), (b) SiO_2-TiO_2 (Ti = 0.1 mol %), and $SiO_2-Al_2O_3-TiO_2$ samples containing 10 mol % of Al and (c) 0.1, (d) 0.25, (e) 0.5, (f) 1.0, and (g) 4.8 mol % of Ti. The spectrum of TiO_2 (h) is also shown.

nm, which is assigned to LMCT (ligand−metal charge transfer) from O to Ti of the isolated tetrahedral TiO_4 in silica matrix.[12,13,39] It is shown that the band edges of the $SiO_2-Al_2O_3-TiO_2$ samples were shifted to longer wavelength beyond 260 nm, suggesting that the addition of Al to the SiO_2-TiO_2 produced a new absorption band or modified the electronic structure of Ti species. All of the $SiO_2-Al_2O_3-TiO_2$ samples of various Al contents exhibited the absorption band in the longer wavelength region than the SiO_2-TiO_2 sample did, and the band shape was varied with the Al contents. To clarify the effect of Al, the difference spectra were obtained by subtraction of the spectrum of the SiO_2-TiO_2 sample (Figure 7A, spectrum b) from those of $SiO_2-Al_2O_3-TiO_2$ samples (Figure 7A, spectra c−f) and shown in Figure 7B. These difference spectra clearly show that the introduction of Al atoms into the SiO_2-TiO_2 system formed an additional absorption band from 220 to 320 nm centered at 245 nm. Taking the band due to Al species (Figure 7a) into account, the additional band would be in the range from 220 to 300 nm. This additional band would be assignable to synergistic absorption sites related to both Al and Ti species. The intensity of the additional band increased with the Al content up to 33 mol % of Al. In addition, it is shown that the absorption around 200 nm corresponding to the isolated TiO_4 species was decreased by the introduction of the Al atoms. This suggests that a kind of new photoabsorption sites is formed by the addition of Al at the expense of the isolated TiO_4 species. Because the wavelength region of the new band (220−300 nm) is similar to that of the Al band (220−320 nm), one might prefer the expression that the addition of a small amount of Ti such

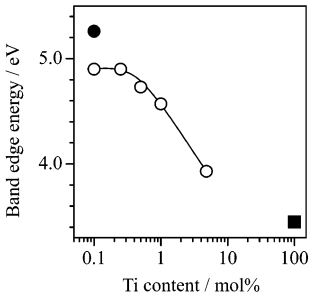

Figure 9. Relation between the edge energy of absorption band and Ti content of the $SiO_2-Al_2O_3-TiO_2$ samples containing 10 mol % of Al (○). The edge energy for the SiO_2-TiO_2 sample (0.1 mol % of Ti, ●) and TiO_2 sample (■) are also plotted.

as 0.1 mol % would enhance the absorption coefficient of the Al species through formation of new synergistic sites.

Figure 8 shows the effect of Ti content on the photoabsorption sites of $SiO_2-Al_2O_3-TiO_2$ samples containing 10 mol % of Al. The $SiO_2-Al_2O_3-TiO_2$ sample with 0.1 mol % of Ti (Figure 8c) exhibited the band in the longer region than that of the SiO_2-TiO_2 sample with the same Ti content (Figure 8b). Because the aggregated Ti species in the SiO_2-TiO_2 system exhibit the band edge in longer wavelength region than that of the isolated TiO_4 species,[14,15,39] one may suspect that the small aggregated Ti species were formed by the Al introduction in the SiO_2-TiO_2 system. However, it is noted that three $SiO_2-Al_2O_3-TiO_2$ samples containing less than 0.5 mol % of Ti exhibited the analogous curve shape of absorption band below 300 nm (Figure 8c−e) though the intensity increased with increasing Ti content. Further increase in the Ti content resulted in the significant red shift of the band over 310 nm (Figure 8f,g), and the band became similar to the band of bulk TiO_2.

The band-edge energy of these spectra was estimated in the same manner as reported,[40] and the results are depicted in Figure 9. The band-edge energy seemed to be constant at lower Ti content than 0.25 mol % and then decreased with increasing Ti content toward the value of bulk TiO_2. The decreasing edge energy in the higher Ti content region would indicate the aggregation of Ti species with an increase of Ti content. However, the constant edge energy at lower Ti content region clearly indicated that the increase of Ti content did not produce the aggregation of Ti species in these samples. Instead of aggregation, the synergistic sites consisting of Al and Ti species would be formed at lower Ti content, which exhibit the additional absorption band centered at 245 nm in the range from 220 to 300 nm.

Because the band edge would be predominantly determined by the absorption species that exhibit the band at longer wavelength, it is difficult to elucidate the presence and variation of the species that exhibit the band at shorter wavelength. Thus, on the sample having aggregated Ti species that exhibit the band at longer wavelength, there is a possibility that the highly dispersed TiO_4 species or the synergistic sites also exist on that sample. However, it seems reasonable that the $SiO_2-Al_2O_3-TiO_2$ sample having aggregated Ti species would scarcely have the highly dispersed TiO_4 species or the synergistic sites because many Ti atoms would be consumed to form the aggregates.

Discussion

Active Pair Sites for the Photoinduced Direct Methane Coupling. In the previous paper, the effect of Al content upon the activity of $SiO_2-Al_2O_3$ was investigated in the photoinduced direct methane coupling.[7] It was demonstrated that the dispersed tetrahedral AlO_4 species, which were dominant in the $SiO_2-Al_2O_3$ samples containing less than 20 mol % of Al, exhibited higher specific activity and selectivity to yield ethane than the aggregated Al species did. In the present study, the ethane yield increased with the Al content until 10 mol % on the $SiO_2-Al_2O_3-TiO_2$ sample having low Ti content less than 1 mol %, while further increase of the Al content decreased the yield (Figure 3). This effect of the Al content of the $SiO_2-Al_2O_3-TiO_2$ system is very similar to the case of the $SiO_2-Al_2O_3$ system. Al K-edge XANES indicates that the tetrahedral AlO_4 species were dominant in the highly active $SiO_2-Al_2O_3-TiO_2$ samples with 10 mol % Al (Figure 5). From these results, it is indicated that the highly active sites for the photoinduced direct methane coupling would be related to the dispersed AlO_4 tetrahedra.

The $SiO_2-Al_2O_3-TiO_2$ sample prepared by the sol−gel method exhibited higher activity than that of the $TiO_2/SiO_2-Al_2O_3$ sample prepared by the impregnation method (Table 1, runs 8 and 10). The Ti K-edge XANES spectra (Figure 6) indicated that the tetrahedral TiO_4 species were major in the sol−gel prepared $SiO_2-Al_2O_3-TiO_2$ samples, while they were minor in the impregnation sample. It is generally accepted that the tetrahedral TiO_4 species are formed when Ti atoms are well dispersed in the silica matrix. From these results, it is proposed that the dispersion of Ti in the catalyst is one of the important factors for exhibiting the high activity in this reaction.

As for the sol−gel prepared $SiO_2-Al_2O_3-TiO_2$ samples with 10 mol % of Al, the introduction of Ti atoms more than 0.5 mol % decreased the activity of $SiO_2-Al_2O_3-TiO_2$ (Figure 3). Judging from the Ti K-edge XANES spectra, the tetrahedral TiO_4 species is dominant in even high Ti samples prepared by sol−gel method. Thus, it is expected that the other structural factors except for the local symmetry of Ti species would also affect the photocatalytic activity. From UV−vis spectra, it was suggested that the decrease of the activity in the high Ti samples would be due to the aggregation of TiO_4 tetrahedra. Or, in other words, the high dispersion of the tetrahedral TiO_4 species in silica matrix is required for the high activity.

The results on the activity in the photoinduced methane coupling clearly showed the synergy effect of the Al and Ti species in silica. The above results suggest that the coexistence of dispersed tetrahedral AlO_4 and dispersed tetrahedral TiO_4 in silica matrix is required for exhibiting high activity of the $SiO_2-Al_2O_3-TiO_2$ sample in this reaction. The difference UV−vis spectra (Figure 7B) show that the addition of Al to the SiO_2-TiO_2 system results not only in the formation of the additional band centered at 245 nm but also in the decrease of absorbance around 200 nm corresponding to the isolated TiO_4 species in the silica matrix.[12,13,39] This suggests that the electronic structure of the isolated TiO_4 species in the silica matrix is affected by the dispersed tetrahedral AlO_4 species and then the new absorption band is created. This new band would be assigned to the synergistic pair sites consisting of the dispersed AlO_4 tetrahedra and highly dispersed TiO_4 tetrahedra. In addition, the band wavelength region, 220−300 nm, is agreed with the effective wavelength for the photoinduced direct methane coupling that was determined to be 210−310 nm by the cut-filter experiments (Table 3). This agreement confirms that these synergistic pair sites are the main active sites for the photoinduced direct methane coupling on the $SiO_2-Al_2O_3-TiO_2$ system.

In Figure 7B, the sample containing 33 mol % of Al showed the maximum intensity of the additional band due to the pair sites among the $SiO_2-Al_2O_3-TiO_2$ samples containing

0.1 mol % of Ti. However, this sample exhibited low activity in the photoinduced direct methane coupling (Figure 3). This means that there are inactive sites exhibiting the additional band at 245 nm, which would be the highly dispersed TiO_4 species combined with aggregated Al oxide species. The dispersion of Al is required as mentioned above.

In the SiO_2-TiO_2 system, the photoabsorption is assigned to LMCT on the $Ti^{4+}-O^{2-}$ moiety of the highly dispersed TiO_4 tetrahedra in silica matrix, which can be also described as LMCT on Ti−O−Si moiety in $Ti(OSi)_4$ species.[12,13,39] Although the structure of the synergistic pair sites has not been clarified yet, one of the most possible structures of this species would be described as $(SiO)_3Ti-O-Al(OSi)_3$ containing the Ti−O−Al moiety. The photoexcitation energy ranged from 4.13 to 5.90 eV (210−300 nm) for the pair sites, which is lower than that for the Ti−O−Si moiety (less than 4.96 eV, 250 nm). Replacement of Si by Al seems to lead a decrease of the photoexcitation energy. This might be explained as the energy level of O^{2-} being higher for the $Ti-O-Al^{3+}$ moiety than for the $Ti-O-Si^{4+}$ moiety. Because the UV light intensity from the light sources in the atmosphere is generally higher at longer wavelength region than the shorter wavelength, the photoactive sites that can be excited by longer wavelength would have an advantage in photoinduced reactions.

The high yield in the photoinduced reaction was obtained over the sample evacuated at high temperature (Figure 4). This suggests that the active pair sites are formed by desorption of surface hydroxyl groups. This is in common among the catalysts for photoinduced direct methane coupling such as $SiO_2-Al_2O_3$,[8,11] zeolite,[10] and the present $SiO_2-Al_2O_3-TiO_2$ systems. Although the active pair sites should be on the surface, the sites would be free from hydroxyl groups, possibly described as $(SiO)_3Ti-O-Al(OSi)_3$.

It is a fact that the best content for Ti (0.5 mol %) was much lower than that for Al (10 mol %). This should be originated from the different properties of Al and Ti. To form the active Ti−O−Al site for the reaction, both Al and Ti species should be well dispersed in the silica matrix. As shown in UV spectra (Figure 7), the introduction of more than 0.5 mol % of Ti resulted in the agglomeration of Ti species. This demonstrates that 0.5 mol % of Ti was upper limit to form the dispersed TiO_4 species in the employed preparation method. On the other hand, Al atom seems much more easily dispersed in silica matrix, that is, a larger amount of the AlO_4 species could be introduced into the silica matrix as dispersed AlO_4 species.[7] To form the largest amount of pair sites consisting of the dispersed AlO_4 and TiO_4 species, it would be required to provide the largest amount of each dispersed species. Thus, the best contents for Al and Ti would be different from each other.

Proposed Reaction Mechanism. Although enough evidences are not shown in the present study, the photoinduced reaction mechanism is discussed briefly here. The LMCT from the lattice oxygen, O_L^{2-}, to Ti^{4+} at the $Ti^{4+}-O_L^{2-}-Al^{3+}$ moiety in the active pair sites would occur upon photoirradiation in the range from 220 to 300 nm to produce photoexcited lattice O_L^- (the hole) and Ti^{3+} (the electron). It is reported that the photoexcited O^- species well abstract hydrogen radical from methane.[4] In addition, it is well-known that the thermally produced O^- species well abstract hydrogen radical from methane to produce ethane, as reported, for example, over Li/MgO catalyst for oxidative coupling of methane.[41,42] On the basis of these aspects, it is proposed that the present photoinduced nonoxidative direct methane coupling would be started from the hydrogen radical abstraction by photoexcited lattice O_L^- species. Judging from the fact of ethane and hydrogen formation, thus produced methyl radicals and hydrogen radicals should be coupled to form ethane and hydrogen molecules, respectively; otherwise, they might be deactivated without product formation. Further investigations are required to confirm the reaction mechanism.

Conclusions

The $SiO_2-Al_2O_3-TiO_2$ ternary oxide system exhibits high photocatalytic activity for the photoinduced nonoxidative direct methane coupling at room temperature. The maximum yield was obtained over the 10 mol % of Al and 0.5 mol % of Ti sample. The highly active sites are the synergistic pair sites consisting of the dispersed AlO_4 and TiO_4 tetrahedra in the silica matrix, such as $(SiO)_3Ti-O-Al(OSi)_3$, which were formed by desorption of the surface hydroxyl groups under the evacuation at high temperature. The photoexcitation at the $Ti^{4+}-O^{2-}-Al^{3+}$ moiety in the active pair sites would occur upon photoirradiation in the range from 220 to 300 nm to activate methane molecules.

Acknowledgment. The authors thank Professor Atsushi Satsuma for the valuable discussion. X-ray absorption experiments at Al K-edge were carried out as the Joint Studies Program (1998) of UVSOR of the Institute for Molecular Science. The X-ray absorption experiment at Ti K-edge was performed under the approval of the Photon Factory Program Advisory Committee (Proposal No. 2001G296). This work was partly supported by a Grant-in-Aid for Scientific Research on Priority Area "Catalytic Reaction Engineering toward Green Chemical Processes" from the Ministry of Education, Culture, Sports, Science and Technology (MEXT), Japan. H.Y. acknowledges the Nitto Foundation and Japan Chemical Innovation Institute (JCII) for financial supports.

References and Notes

(1) Xu, Y.; Lin, L. *Appl. Catal. A* **1999**, *188*, 53.
(2) Gesser, H. D.; Hunter, N. R. *Catal. Today* **1998**, *42*, 183 and references therein.
(3) Okabe, K.; Sayama, K.; Kusama, H.; Arakawa, H. *Chem. Lett.* **1997**, 457.
(4) Kaliaguine, S. L.; Shelimov, B. N.; Kazansky, V. B. *J. Catal.* **1978**, *55*, 384.
(5) Kuzmin, G. N.; Knatko, M. V.; Kurganov, S. V. *React. Kinet. Catal. Lett.* **1983**, *23*, 313.
(6) Hill, W.; Shelimov, B. N.; Kazansky, V. B. *J. Chem. Soc., Faraday Trans. 1* **1987**, *83*, 2381.
(7) Yoshida, H.; Matsushita, N.; Kato, Y.; Hattori, T. *Phys. Chem. Chem. Phys.* **2002**, *4*, 2459.
(8) Yoshida, H.; Kato, Y.; Hattori, T. *Stud. Surf. Sci. Catal.* **2000**, *130*, 659.
(9) Kato, Y.; Yoshida, H.; Hattori, T. *Chem. Commun.* **1998**, 2389.
(10) Kato, Y.; Yoshida, H.; Hattori, T. *Microporous Mesoporous Mater.* **2002**, *51*, 223.
(11) Kato, Y.; Yoshida, H.; Hattori, T. *Phys. Chem. Chem. Phys.* **2000**, *2*, 4231.
(12) Anpo, M.; Aikawa, N.; Kubokawa, Y.; Che, M.; Louis, C.; Giamello, E. *J. Phys. Chem.* **1985**, *89*, 5017.
(13) Yamashita, H.; Kawasaki, S.; Ichihashi, Y.; Harada, M.; Takeuchi, M.; Anpo, M.; Stewart, G.; Fox, M. A.; Louis, C.; Che, M. *J. Phys. Chem. B* **1998**, *102*, 5870.
(14) Murata, C.; Yoshida, H.; Hattori, T. *Stud. Surf. Sci. Catal.* **2002**, *143*, 845.
(15) Murata, C.; Yoshida, H.; Kumagai, J.; Hattori, T. *J. Phys. Chem. B* **2003**, *107*, 4364.
(16) Anpo, M.; Chiba, K. *J. Mol. Catal.* **1992**, *74*, 207.
(17) Yamashita, H.; Ichihashi, Y.; Anpo, M.; Hashimoto, M.; Louis, C.; Che, M. *J. Phys. Chem.* **1996**, *100*, 16041.
(18) Zhang, S. G.; Fujii, Y.; Yamashita, H.; Koyano, K.; Tatsumi, T.; Anpo, M. *Chem. Lett.* **1997**, 659.
(19) Yoshida, H.; Murata C.; Hattori, T. *Chem. Commun.* **1999**, 1551.
(20) Ulagappan, N.; Frei, H. *J. Phys. Chem. A* **2000**, *104*, 7834.
(21) Tanaka, T.; Teramura, K.; Yamamoto, T.; Takenaka, S.; Yoshida, S.; Funabiki, T. *J. Photochem. Photobiol. A* **2002**, *148*, 277.

(22) Kato, Y.; Matsushita, N.; Yoshida, H.; Hattori, T. *Catal. Commun.* **2002**, *3*, 99.
(23) Yoshida, H.; Murata, C.; Hattori, T. *J. Catal.* **2000**, *194*, 364.
(24) Uchijima, T. In *Catalytic Science and Technology*; Yoshida, S., Takazawa, N., Ono, T., Eds.; Kodansha VCH: Tokyo, 1991; Vol. 1, p 393.
(25) Kato, Y.; Shimizu, K.; Matsushita, N.; Yoshida, T.; Yoshida, H.; Satsuma, A.; Hattori, T. *Phys. Chem. Chem. Phys.* **2001**, *3*, 1925.
(26) Yoshida, H.; Chaskar, M. G.; Kato, Y.; Hattori, T. *J. Photochem. Photobiol. A*, in press.
(27) Nomura, M.; Koyama, A. *J. Synchrotron Radiat.* **1999**, *6*, 182.
(28) Nomura, M.; Koyama, A. *Nucl. Instrum. Methods Phys. Res., Sect. A* **2001**, *467*−*468*, 733.
(29) Yoshida, T.; Tanaka, T.; Yoshida, H.; Funabiki, T.; Yoshida, S. *J. Phys. Chem.* **1996**, *100*, 2302.
(30) Murata, T.; Matsukawa, T.; Naoe, S.; Horigome, T.; Matsuo, O.; Watanabe, M. *Rev. Sci. Instrum.* **1992**, *63*, 1309.
(31) Takata, Y.; Shigemasa, E.; Kosugi, N. *J. Synchrotron Rad.* **2001**, *8*, 351.
(32) McKeown, D. A.; Waychunas, G. A.; Brown, G. E., Jr. *J. Non-Cryst. Solids* **1985**, *74*, 349.
(33) Cabaret, D.; Sainctavit, P.; Ildefonse, P.; Flank, A.-M. *J. Phys.: Condens. Matter*. **1996**, *8*, 3691.
(34) Fröba, M.; Tiemann, M. *Chem. Mater*. **1998**, *10*, 3475.
(35) Van Bokhoven, J. A.; Sambe, H.; Ramaker, D. E.; Koningsberger, D. C. *J. Phys. Chem. B* **1999**, *103*, 7557.
(36) Frages, F.; Brown, G. E., Jr.; Rehr, J. J. *Phys. Rev. B* **1997**, *56*, 1809.
(37) Bordiga, S.; Coluccia, S.; Lamberti, C.; Marchese, L.; Zecchina, A.; Boscherini, F.; Buffa, F.; Genoni, F.; Leofanti, G.; Petrini, G.; Vlaic, G. *J. Phys. Chem.* **1994**, *98*, 4125.
(38) Kim, W. B.; Choi, S. H.; Lee, J. S. *J. Phys. Chem. B* **2000**, *104*, 8670.
(39) Gao, X.; Bare, S. R.; Fierro, J. L. G.; Banares, M. A.; Wachs, I. E. *J. Phys. Chem. B* **1998**, *102*, 5653.
(40) Luca, V.; Djajanti, S.; Howe, R. F. *J. Phys. Chem. B* **1998**, *102*, 10650.
(41) Ito, T.; Lansford, J. H. *Nature* **1985**, *314*, 721.
(42) Ito, T.; Wang, J.; Lin, C.; Lansford, J. H. *J. Am. Chem. Soc.* **1985**, *107*, 5062.